Journal of Hydrology: Regional Studies 49 (2023) 101506

Contents lists available at ScienceDirect

Journal of Hydrology: Regional Studies

journal homepage: www.elsevier.com/locate/ejrh

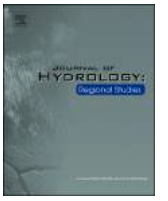

The role of residual risk on flood damage assessment: A continuous hydrologic-hydraulic modelling approach for the historical city of Rome, Italy

A. Fiori [a,*], C.P. Mancini [a], A. Annis [b], S. Lollai [a], E. Volpi [a], F. Nardi [b], S. Grimaldi [c]

[a] DICITA, Roma Tre University, Rome, Italy
[b] WARREDOC, University for Foreigners of Perugia, Perugia, Italy
[c] DIBAF, University of Tuscia, Viterbo, Italy

ARTICLE INFO

Keywords:
Flood risk
Residual risk
Continuous modelling
Rome
Tiber river
Historical city

ABSTRACT

Study region: The municipality of Rome (Italy) and the Middle Tiber River valley.
Study focus: Ordinary and residual flood risk assessment is a crucial topic in hydrology with a variety of practical implications for improving the extreme event management. Nowadays and in such context, the continuous hydrological-hydraulic modelling is an emerging approach and this study supports the conclusion that it can provide a very informative flood risk assessment. Moreover, when the study domain includes relevant and very expensive historical centers, like Rome, such methodology allows for a complete characterization of the risk providing the necessary information for decision-makers.
New hydrological insights for the region: In the present work we illustrate an exhaustive flood risk assessment, quantifying the benefits of applying the hydrologic-hydraulic continuous modelling approach. Specifically, we verify that in the city of Rome flooding begins with events of 175 years return period which generates damage of hundreds of million euro. The flood-damage relationship as a function of return period, then, grows linearly up to floods with a return period of around 350 years, for which the majority of the historical town is flooded; then the estimated damages keep growing with the return period to reach a damage of about ten billion euros for 500 years flood events.

1. Introduction

Flood risk is the combination of the probability of occurrence of an inundation event and the potential adverse consequences for human health, for civil infrastructures and assets, for natural ecosystems, for cultural heritage and the wide spectra of economic and social activities that develop along floodplains (EU Floods Directive, 2007 / 60 EC). The effectiveness of flood hazard mitigation infrastructures shall be evaluated by cost-benefit analyses, as required by the EU Floods Directive, quantifying the socio-economic impacts of flooding. Standard approaches for engineering design and identification of optimal flood protection measures require a quantitative assessment of flood risk as a function of hydrological forcing scenarios (rainfall and distributed runoff scenarios) and comparative quantifications of impacts on floodplain functions and assets by the planned infrastructure (Metin et al., 2020).

* Corresponding author.
E-mail address: aldo.fiori@uniroma3.it (A. Fiori).

https://doi.org/10.1016/j.ejrh.2023.101506
Received 8 March 2023; Received in revised form 2 August 2023; Accepted 11 August 2023
Available online 16 August 2023

Following the approach outlined by Varnes (1984), risk R is defined as the product of hazard H, i.e. the probability of the event occurring in a specific time interval and area (usually expressed in terms of return period scenario), elements at risk C, and vulnerability V, defined as the rate of the element at risk that is damaged (ranging between 0 and 1), such that risk can be written as $R = H\,V\,C = H\,D$, with $D = V\,C$ the damage.

Varnes' formula can be generalized, and risk can be estimated as the expected value of damage (Merz et al., 2010) after knowledge of the probability distribution of the random variables describing the hydrological forcing, typically fluvial discharge or water depth. Although damage assessments can be associated to several hydrologic, geomorphic and biogeochemical governing factors (e.g. flow velocity, flooding duration, sediment and contaminant transport, to mention a few), typically the main driving variable for its quantification is the water depth within the flooded area (e.g., D'Angelo et al., 2020). For simplicity, here, we assume a bijective relationship between damage D and the water depth h at a generic location $\boldsymbol{x}$, such that $D = D(h)$ in the same location (i.e. water depth-damage curve). Adopting this assumption, Varnes' formula can be written as

$$R(x) = E[D] = \int_0^1 D(h)P_h \tag{1}$$

where P_h is the cumulative density function (cdf) of the maximum water depth at location $\boldsymbol{x}$ and P_h and $D(h)$ quantities depend on the specific location $\boldsymbol{x}$.

The quantity of interest in most applications of flood risk analysis is the aggregated risk over a certain area of interest A (R_A). The aggregated risk $R_A$can be calculated from by integration of Eq.(1) over the area A

$$R_A = \int_A R(x)dx \tag{2}$$

The residual risk is also crucial for flood risk management plans, being defined as "the risk that remains in unmanaged form, even when effective disaster risk reduction measures are in place, and for which emergency response and recovery capacities must be maintained" (UNISDR, 2009). In practice, the residual risk is related to probability that exceeds the safety value established through Eqs. (1) and (2), i.e. the return period for the design of flood protection measures; it is useful to verify that the design return period is appropriate for an effective flood risk protection plan (Galloway et al., 2005; Bell and Tobin, 2007; Ludy and Kondolf, 2012; Pinter et al., 2016).

Along Eqs. (1, 2), the determination of risk R_A requires the knowledge of both P_h and $D(h)$ at each location $\boldsymbol{x}$ within the area A of interest. They depend on the complex interaction between the flood event and the river/floodplain system - including the assets value or exposure and their vulnerability - together with the climatic forcing and associated frequency.

The quantities describing flood hazard P_h and $D(h)$ are typically derived through suitable hydrological-hydraulic models. The hydrological forcing information cannot be limited to the peak discharge since the flood hydrograph duration, volume and shape play important roles for an appropriate characterization of water depth in the area of interest. Furthermore, standard event-based design flood hydrograph estimation approaches, based on critical rainfall amount and the related design hyetograph, could be also impacted by relevant uncertainties considering some incoherent assumptions that tend to underestimate hydrograph volumes that represent governing factors of flood extent and depth estimations. The continuous-time simulation (Boughton and Droop, 2003; Hoes and Nelen, 2005; Fleischmann et al., 2019; Beneyto et al., 2020; Grimaldi et al., 2013, 2021, 2022), employed in this work, allows to overcome main limitations of hydrological design event-based approaches (as e.g. discussed in Grimaldi et al., 2012; Cipollini et al., 2021) also addressing hydro-modelling chain uncertainties (Annis et al., 2020), leaving the lumped hydrograph concept towards the production of a large sample of simulated hydrographs mimicking the natural wide spectra of flood realizations. The proposed continuous approach implements a cascade simulation of rainfall, rainfall-runoff and flood routing dynamics resulting in a naturally continuous rainfall-driven distributed river flow generation occurring over thousands of years, surrogating to the lack of observations of historical time series associated to rare and extremely rare events, at least up to 500 years of return time (i.e. the low probability flood, or extreme event scenario according to the Italian legislation enacting the EU Flood Directive). The continuous hydro-modelling chain is, then, completed by the implementation of an accurate hydraulic model (possibly a 2D flood routing model considering the out-of-channel floodplain distributed dynamics associated to extreme events) for the propagation of floods.

The present work describes the risk analysis of the city of Rome (Italy) as exposed to floods of the Tiber River. This flood risk analysis is of paramount importance considering the relevance of Rome, host of the main political institutions of Italy, UNESCO World Heritage Site and third most populous city in Europe (SwissRe, 2023). Likely, a large amount of hydrological and hydraulic information, including historical information, are available for the Tiber-Rome case study, as described in the following Section 2. Of particular interest for this work is the role played by the North Tiber river reach in the immediate upstream portion of the Rome metropolitan area, namely the Middle Tiber Valley (MTV), that have a significant flood wave attenuation effect and, consequently, constitutes a flood risk mitigation factor for Rome. Managing urban infrastructures and land use change in the MTV is a crucial floodplain planning action since any landscape change may have direct effects in increasing the flooding hazard for the city of Rome.

To the best of our knowledge this is the first research investigating on a large scale quantification of the flood risk of Rome and Tiber river floodplains, as well as the first analysis in this study area adopting the continuous-simulation methodology. This was possible thanks to the large amount of historical and recent Tiber flood studies available (Calenda et al., 2009; Mancini et al., 2022) as well as to the maturity of continuous hydrologic-hydraulic modelling applications at large scales. Moreover, the peculiar aspect of the study is related to the role of the residual risk in Rome which represents a governing factor for appropriate risk assessment and mitigation engineering works for protecting this valuable historical domain (Arrighi et al., 2013; Galloway et al., 2020).

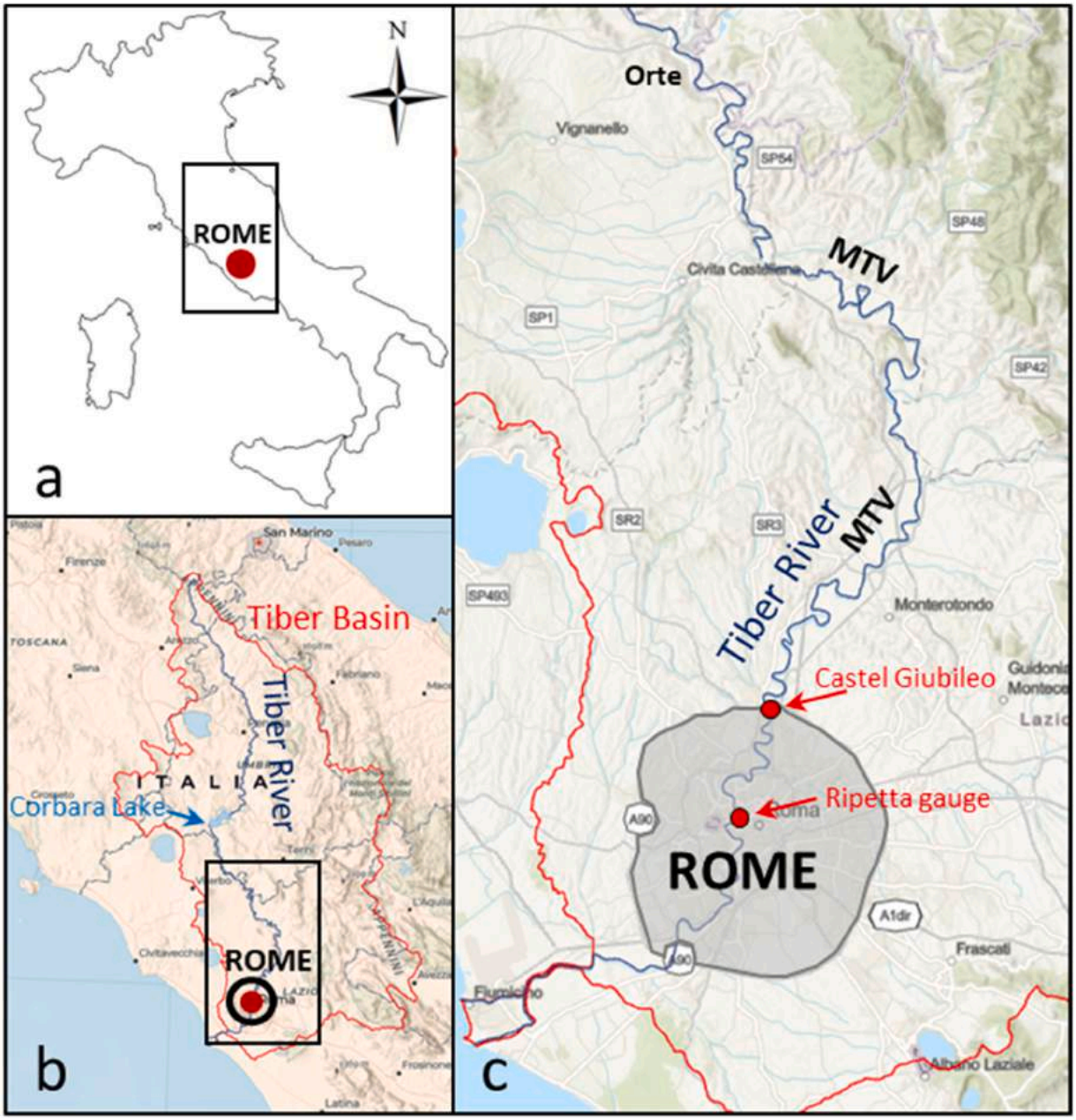

Fig. 1. The study area with three focus maps from the Italy-scale geographic location of the city of Rome (panel a) the Tiber River basin domain (panel b) and the zoomed region of Rome and the Middle Tiber River Valley (MTV) (panel c).

In the following sections we describe the material and methods available for this research with specific regard to the hydrological and hydraulic modelling approaches employed for the determination of the probability distribution of the damage (Section 2). Then, in Section 3, results are shown related to the quantification of the risk analysis, while in Section 4 some discussion is provided, particularly on residual risk and the benefit of assessing normalized risk for the study case. Conclusive remarks are finally closing the paper.

2. Materials and methods

2.1. Site description

The Tiber River basin, draining an overall area of roughly 17,500 km^2 with a concentration time of approximately 6 days, lies in Central Italy including the city of Rome (see Fig. 1), the capital and largest city in Italy where several inundation events occurred in the

past, reported over the centuries (e.g. Calenda et al., 2009; Mancini et al., 2022). The Tiber river has an average slope along the MTV equal to 0.01%, while in the city it is 0.02%. The levee-protected river is 100 m large on average within the historical city, while its upstream valley is characterized by larger floodplain widths (about 2500 to 4000 m in MTV). The peak discharges observed in Rome are relatively small if compared with those of other similar or smaller basins; this is largely due to the extensive flooding, and consequent attenuation of flood discharges and volumes, occurring upstream in the MTV and along major tributaries, between the city of Orte and Rome (Fig. 1c).

Available studies suggest that Rome is not affected by flood events with a return period (hereinafter T_r) less then 100–200 hundred years, while the MTV is flooded by events with smaller return periods, approximately in the range 20–30 years. This is because the MTV floodplain is not disconnected, while a system of levees (from Castel Giubileo to the river mouth, Fig. 1c) supports the hydraulic protection of the city of Rome for events with return period of approximately 175 years or lower (as by available studies and further investigated in this work). Therefore, the MTV has a paramount importance in the protection of Rome from floods thanks to the upstream storage effect produced by the relatively frequent inundation of the valley, that reduces the peak discharge downstream (Mancini et al., 2022). Indeed, in recent years, flood events occurred in 2005, 2010 and 2012 have only partially inundated the Middle Tiber Valley (MTV) while the city of Rome wasn't affected at all (Annis et al., 2022).

2.2. Methodology

The proposed flood risk assessment procedure, providing a numerical solution of Eqs. (1–2), relies on the following steps, illustrated in detail in the subsequent sections:

1. Hydrological simulation based on continuous-time simulation (Section 2.3):
   a. simulation of 20,000 years of synthetic rainfall distributed over the Tiber River catchment (Fig. 1b);
   b. estimation of the corresponding flood annual maxima events through rainfall-runoff modeling over the catchment and flood routing along the main river network;
   c. estimation of the empirical probability distribution of all the 20,000 events at all the cross sections of interest (e.g. Castel Giubileo, Fig. 1c).

1. 1D/2D hydraulic simulation (Section 2.4): propagation of 100 flood events (characterized by their return period values pertaining to the empirical distribution at step 1.c) along the Tiber River, in both the MTV and the city of Rome.
2. Damage estimation for each of the 100 flood events, based on distributed water levels in the 2D floodplain domains and literature stage-level relationships (Section 2.5).
3. Risk estimation (Section 2.6): reconstruction of the probability distribution of damage, assuming for simplicity that the probability of damage equals the corresponding flood peak and risk estimation in MTV and the city of Rome.

2.3. Hydrological modeling using a continuous simulation approach

Flood hydrographs at several Tiber cross sections within the floodplain study domain are available as calculated by the hydrological model of the Central Apennine District Basin Authority (ABDAC, 2003). The ABDAC model schematizes the Tiber basin as composed of 40 subbasins characterizing the rainfall-runoff transformation of the Upper Tiber and its main tributaries. Flood routing along the Tiber, from Corbara reservoir (depicted in Fig. 1b) to the sea, is modeled by a one-dimensional (1D) flow routing model. Rainfall distribution fields for the catchment are associated with nine homogeneous areas. For these nine regions, 20,000 years of synthetic rainfall time series at hourly resolution are generated. The rainfall generator is calibrated by available intense rainfall observations in the area, while the rainfall-runoff and flow routing modelling components are calibrated using the several observed flood events for the city of Rome (1937, 1965, 1969, 1976, 1979, 1984, 1992, 1997 and 1998). Among those flood events, the 1937 and 1965 floods are considered very rare events while exceeding 2550 m^3/s, corresponding to the water level of 16 m at the ancient Ripetta gauge in Rome (Fig. 1c), meaning that the city would have been inundated before the levee system was completed. Other events seem to be less severe, yet generally exceeding the peak value of 1500 m^3/s in Rome (Ripetta).

Assuming stationarity, the model reproduces satisfactorily the statistical behavior of peak discharge as observed at Ripetta gauge, at least in the range of return period values considered here, with a slight underestimation of flood peak for $T_r < 100$ years. Despite the stationary condition assumed here, climate change could be included in the proposed hydro-modelling framework, e.g., allowing for a changing behavior of the simulated rainfall field and of temperature values ruling evapotranspiration and humidity conditions.

In the present study, the ABDAC model is employed for (i) the calculation of the peak discharge cdf (P_Q), as required by the flood risk procedure, and (ii) to provide a series of flow hydrographs, with different frequency of occurrence, to be propagated over the MTV and the city of Rome. In particular, 100 events are extracted from the upper tail of the discharge P_Q, which is made up of 20,000 years of simulations, as representative values of the peak discharge for a variety of return periods, starting from approximately $T_r = 20$ years. The selected events are the reference flood events provided to flood practitioners by ABDAC to delineate the flood prone areas along the Tiber river upstream and in the city of Rome. More specifically, each of the 100 events is selected as the maximum flood (in terms of peak discharge) of a 200-year period extracted from the 20,000 years one at Ripetta gauge. This means that the 100 events are not the largest 100 events among the 20,000, and that the selected events might represent the sampling variability of the $T_r = 200$ year flood event, when statistically interpreted under a different perspective. It is also interesting to stress that, while being characterized by very

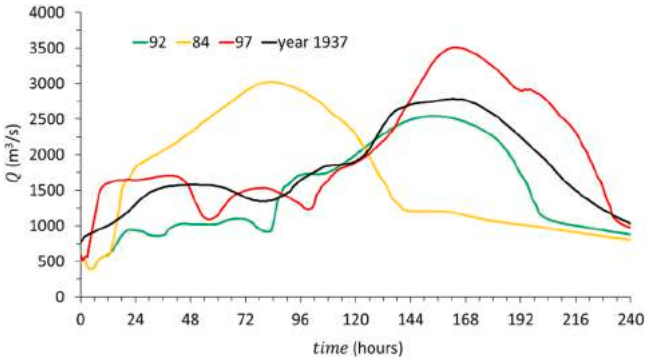

Fig. 2. Exceptional flood event occurred in 1937 with three of the synthetic hydrographs simulated by using the ABDAC hydrological model, 84, 92 and 97 floods, at Rome-Ripetta.

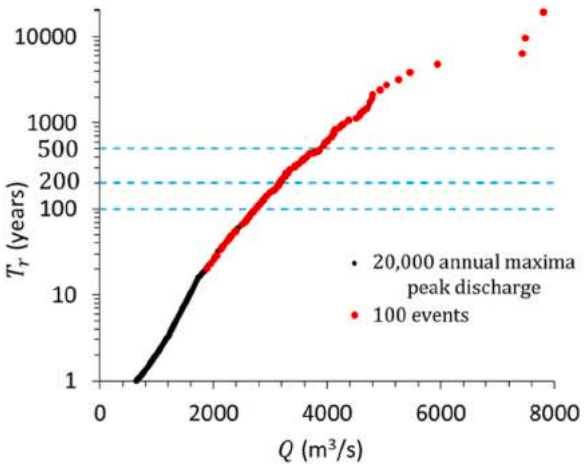

Fig. 3. Empirical return period of peak discharge for all the 20,000 synthetic events (solid black circles) simulated by using the ADBAC model and for the 100 selected events (red circles) at Rome-Ripetta.

different shapes, the 100 events depict a strong correlation coefficient between peak discharge and volume (not shown here for the sake of brevity), as for the observed events at the Ripetta gauge (Volpi and Fiori, 2012). Fig. 2 compares three of the 100 synthetic hydrographs simulated by using the ABDAC hydrological model, 84, 92 and 97 as indicated by progressive numbering, also showing the exceptional flood event occurred in 1937.

Fig. 3 shows the empirical return period as a function of the peak discharge Q at the Ripetta cross-section (central Rome, see Fig. 1c) for the 20,000 annual maxima considered, including the 100 events that are employed in the flood risk assessment, as described above. We remark that the 100 hydrographs display a rather wide range of shapes, as a function of the simulated precipitation patterns. Such variety of hydrological forcing lies at the heart of the continuous modeling approach, that aims at representing the natural hydrological variability as realistically as possible, with all the possible varying precipitation scenarios and basin responses.

2.4. Hydraulic modeling and calibration

The risk assessment requires a detailed representation of peak discharge and water depth distributions in the MTV and the city of Rome, with specific regard to the Tiber floodplain within the city historical center. A two-dimensional (2D) unsteady flow hydraulic model is, thus, implemented from the Nazzano barrage, which is the upper limit of the MTV, to the river mouth (Thyrrennian Sea). Fig. 4 displays the computational domain. This large scale distributed 2D model is split in two simulation sub-domains for computational efficiency, representing the flow dynamics in respectively the Nazzano barrage to the Castel Giubileo barrage (just upstream Rome) and the Castel Giubileo to the river mouth, that also include the Aniene River, a major lateral Tiber tributary within the Rome urban domain (Fig. 4). The hydraulic model is implemented by means of the HEC-RAS software (Brunner, 2016), integrating a 1D, de Saint Venant formulation for the riverbed and a 2D parabolic model for the flooded areas. The upstream boundary condition (Nazzano) and the inflow from MTV tributaries are associated to the hydrographs produced by the 100 simulations of ABDAC model (Section 2.2). Same method for boundary conditions for the Rome model, apart from the upstream condition that is taken from the upstream 2D model of the MTV. The downstream boundary conditions are the stage-discharge relationships at the Castel Giubileo cross section for

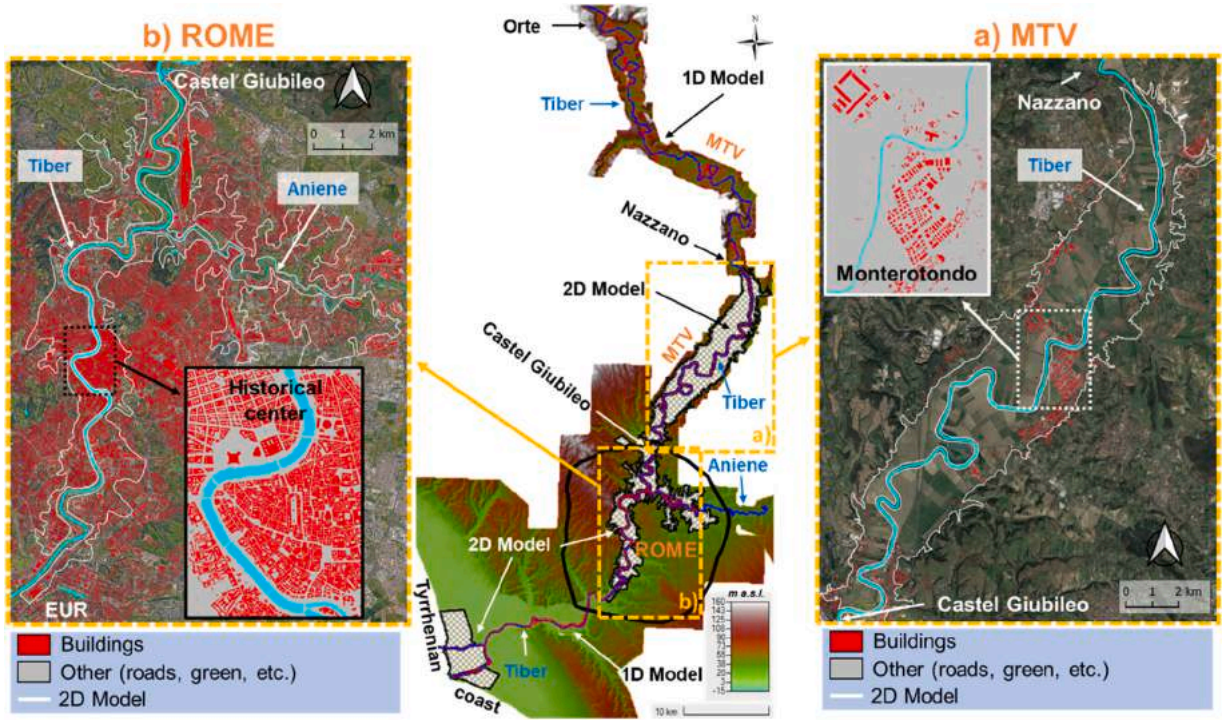

Fig. 4. Computational domain of the two-dimensional hydraulic models: a) Tiber River from Nazzano to Castel Giubileo; b) Tiber and Aniene Rivers from Castel Giubileo to the mouth and from downstream of Lunghezza to the confluence with the Tiber, respectively.

the MTV 2D model and the storm surge level (0.75 m a.s.l. as in Mancini et al., 2022) for the 2D model of the city of Rome.

The floodplain geometry of the hydraulic model is implemented by merging available topographic datasets including the LiDAR Digital Elevation Map (resolution 1x1m) from the Ministry of the Environment. Overall the Tiber hydro-topographic model for the entire study domain employs: (i) for the MTV area a river stretch about 40 km long, with 187 river sections and about 200,000 2D cells, with size ranging from 25 m^2 (cells 5x5m) to 400 m^2 (cells 20x20m), as required by the topography (2D domain of about 70 km^2); (ii) for the second area, from Castel Giubileo to the mouth and the Aniene River, two river reaches of about 56 km and 11 km, respectively, with 640 river sections and approximately 3350,000 cells, with size 25 m^2 (2D domain of approximately 84 km^2). To ensure the stability and accuracy of numerical simulations the computational time was assumed equal to 10 and 15 s the MTV and city of Rome domains, respectively. The mass error is negligible in both cases being generally less than 1%.

The calibration of the 1D hydraulic model is performed by simulating a few significant events, including the recent and highly monitored flood occurred in 2012. The resulting 1D roughness parameter values expressed in terms of Manning coefficient are $n_c = 0.037\ m^{-1/3}s$ in the riverbed and $n_f = 0.060\ m^{-1/3}s$ in the floodplains for MTV, $n_c = 0.04\ m^{-1/3}s$ and $n_f = 0.023 - 0.05\ m^{-1/3}s$ in the urban area of Rome and $n_c = 0.03\ m^{-1/3}s$ and $n_f = 0.045\ m^{-1/3}s$ downstream to the river mouth. Roughness parameter definition for the 2D out-of-channel distributed urban domain is challenging since the river did not experience flooding from the beginning of the XX century, due to the realization of the flood defense measures in the city; the calibration is done by reproducing the last and accurately monitored extreme flood occurred in Rome in December 1870, modeled in Mancini et al. (2022), adjusting the changing topography for the actual floodplain morphology. Mancini et al. (2022) introduced a street roughness, n_s, which takes into account the distributed head losses along the streets and the localized head losses at the crossings, and a much larger roughness n_b to simulate the slow movement of water through the buildings. The roughness parameters of the 2D urban domain are $n_s = 0.06\ m^{-1/3}s$ for street roughness and $n_b = 100\ m^{-1/3}s$ for building roughness.

The 2D numerical flood model, fed by the 100 food hydrographs simulated by the ABDAC hydrological model, provides a detailed spatial description of the maximum discharge Q and the maximum water depth h, that are estimated for each of the 3,550,000 cells of the numerical domain. The flood damage assessment and the related depth-damage curve is illustrated in the next subsection.

2.5. Depth-damage curve

As discussed in the Introduction, the flood damage is usually determined using depth-damage curves, which represent the flood damage that would occur at specific water depths per asset or per land-use class. Unfortunately, such curves are not available for many regions, and methodologies usually differ within countries (Molinari et al., 2020). For this reason, a global and consistent database of depth-damage curves has been developed and elaborated by Joint Research Center (JRC) of the European Commission, and the results are presented in the Technical Report by Huizinga et al. (2017). The database has been extensively employed in several studies over the

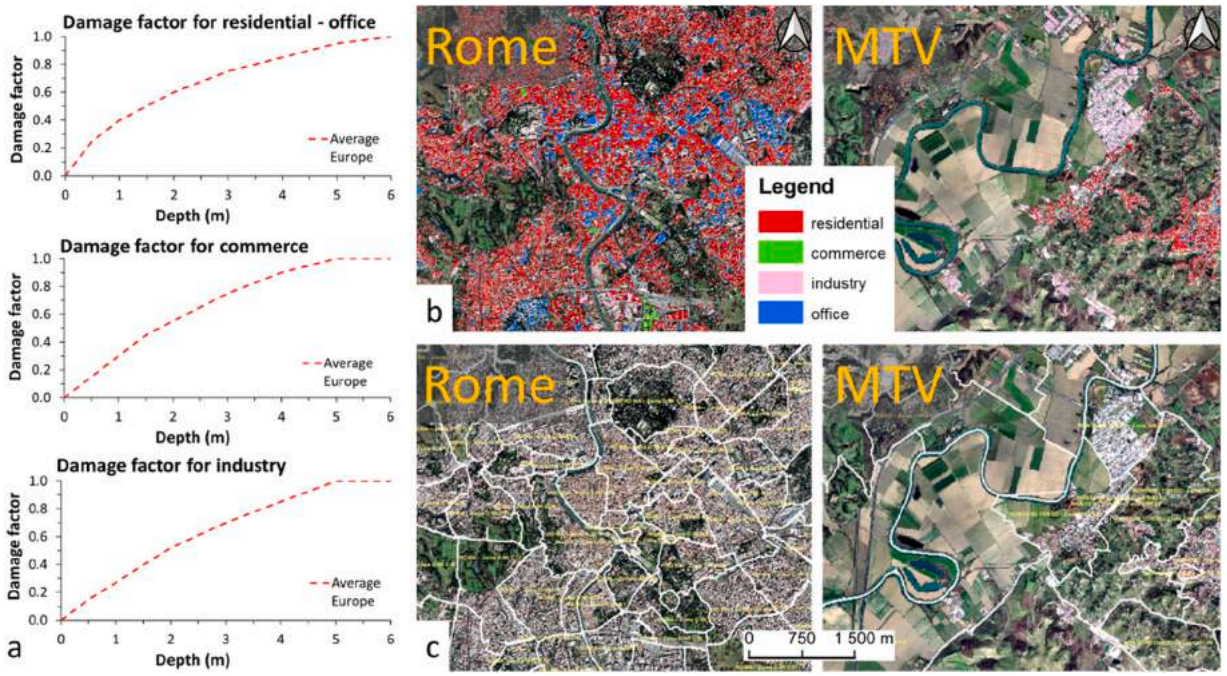

Fig. 5. a) Depth-damage factor curves in Europe for different types of buildings (Huizinga et al., 2017); b) shape file of the buildings (NCTR Lazio Region, 2014); c) zoning of the territory with real estate prices of buildings based on their type of use (Trends in Italian real estate market, Italian Revenue Agency, 2020).

years (see, e.g., Bates, 2022; Merz et al., 2021; Paprotny et al., 2021). Based on an extensive literature survey, normalized damage curves have been developed for each continent, while differences in flood damage among countries is set by determining maximum damage values at the country scale.

As no damage model is currently available in the presented study case, the above mentioned reference dataset for depth-damage assessments is employed. We emphasize that, along the JRC report, only direct, tangible direct damage to buildings has been considered, thus not considering other types of exposed elements (linear infrastructures, crops, historical and archaeological assets, etc.). Similarly, tangible indirect damage (loss of economic activity, additional civil protection costs, loss of property value, insurance costs, etc.) and intangible damage (loss of human life, environmental, archaeological, etc.) are not considered here. Hence, the damage analyzed in this study should be considered an underestimation of the overall damage, providing a simple and highly approximated estimate. Nevertheless, the resulting flood risk can be very effective and helpful when comparing flooding conditions in different geographic areas, as it is done here, or to compare different design options for flood protection measures (an example shall be given in Section 4). We advocate that, although all the mentioned uncertainties, such "comparative" use of flood risk is rather robust and it may lead to meaningful comparisons of scenarios.

For flood-damage assessment of urban features, four types of buildings are considered: residential, commercial, industrial, and offices, that are prevalent in the area under examination. Therefore, other types (i.e. ones pertaining to recreational, sports, military, and agricultural activities), that are not frequently found in the study case, have not been considered. To determine the urban feature economic value as assets exposed to flood damage, the shape files of building footprints (Fig. 5b) and related real estate prices in €/m^2 (Fig. 5c) are used. The European averages of the depth-damage curves are adopted (Fig. 5a) as elaborated in the Technical Report by Huizinga et al. (2017).

In line with the methodology set out in the aforementioned JRC Technical Report, it is then assumed:

- for the building structures: (i) only a net area equal to 85% of the total one is considered for damage computation, and (ii) 40% of the structure is assumed to be not damageable (reinforced concrete and/or masonry buildings);
- for the assets contained in the exposed buildings: (i) only 50% of the assets is damaged for residential and office buildings, (ii) 100% for commercial buildings, and (iii) 150% for industrial buildings.

For additional details on the procedure to apply the aforementioned curves, the readers are referred to Huizinga et al. (2017).

Finally, considering that shapefiles of the buildings represent only the perimeter of the whole commercial structure (shopping centers, wholesale distributors, etc.), based on the analysis of the list of commercial activities (see Register of the Municipality of Rome), it is estimated that on average the surface of buildings with residential use is made up of 30% commercial activities (i.e. shops).

The application of this procedure, employing the water depth data from the simulation of the 100 flood events by the hydrologic/hydraulic modeling chain, leads to the determination of the risk for both the MTV and Rome, denoted hereinafter as R_{MTV} and R_{RM},

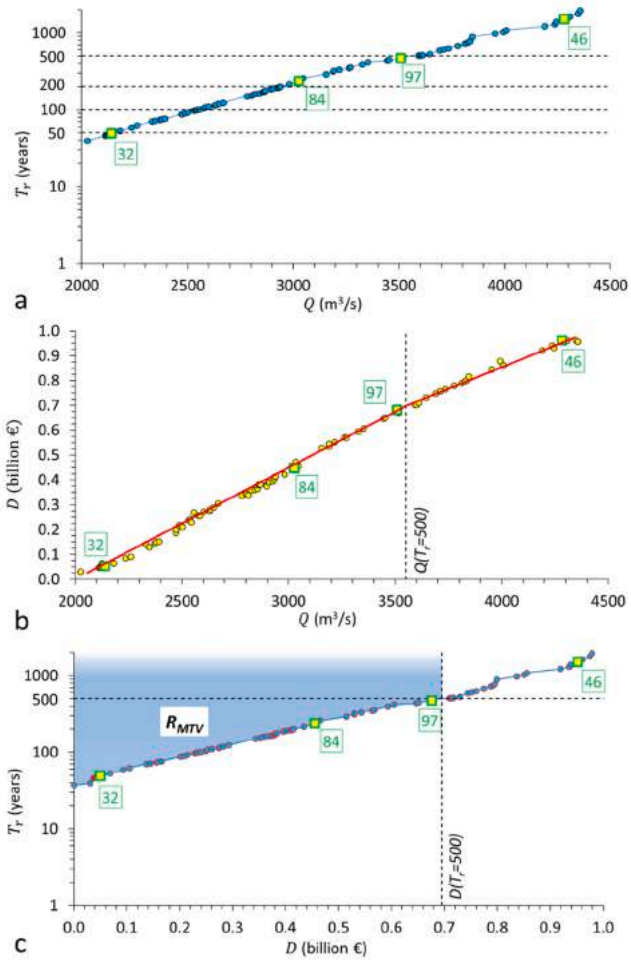

Fig. 6. (a) Probability distribution of flood peak discharge at the Castel Giubileo reference section; (b) simulated flow-damage relationship at the MTV; (c) probability distribution of damage at the MTV, where the colored area represents the flood risk (i.e. the expected annual damage). Only the events flooding the MTV are reported in the figure. A few significant flood events out of the 100 employed are marked in green in all the panels; note also that in panels b and c the vertical dashed line identifies the discharge and damage corresponding to the maximum return period value considered in the analysis, $T_r = 500$ years.

respectively.

2.6. Risk estimation

Given the complexity of the presented modeling approach (large 2D domains, 100 simulations for each model) and the consequent large computational times, the proposed risk assessment procedure is simplified as follows. Instead of deriving P_h and $D(h)$ for all cells of the 2D models, the aggregated damage D, the frequency of the aggregated damage D is calculated as associated to the frequency of the 100 flooding events at a suitable reference section, representative of the domain under consideration. Note that, following Grimaldi et al. (2013), the adopted approach is more advanced than a semi-continuous approach, where synthetic hydrographs are estimated using the peak discharge as the driving variable for each return period and the hydrograph shape is a-priori defined. Nonetheless the implemented approach is less advanced as respect to the fully-continuous approach, considering that the entire runoff time series is not fully injected into the hydraulic flood routing model, but only selected flood events. Such approach leads to a considerable reduction of computational times, at the cost of decreasing estimation accuracy. In general, the discharge return period is not always representative of the damage return period, as shown by Falter et al. (2015); this is, however, not a significant issue as the estimate of D is itself prone to a significant degree of uncertainty, as previously discussed.

The risk assessment is performed assuming as reference the Castel Giubileo cross section, which corresponds to the downstream boundary condition of the 2D model of the MTV and the upstream boundary condition of the 2D model of Rome. Selecting a different reference section within the Tiber reach of interest does not significantly affect the results.

The risk assessment is derived by analyzing events that inundate both MTV and Rome; such events are characterized by return

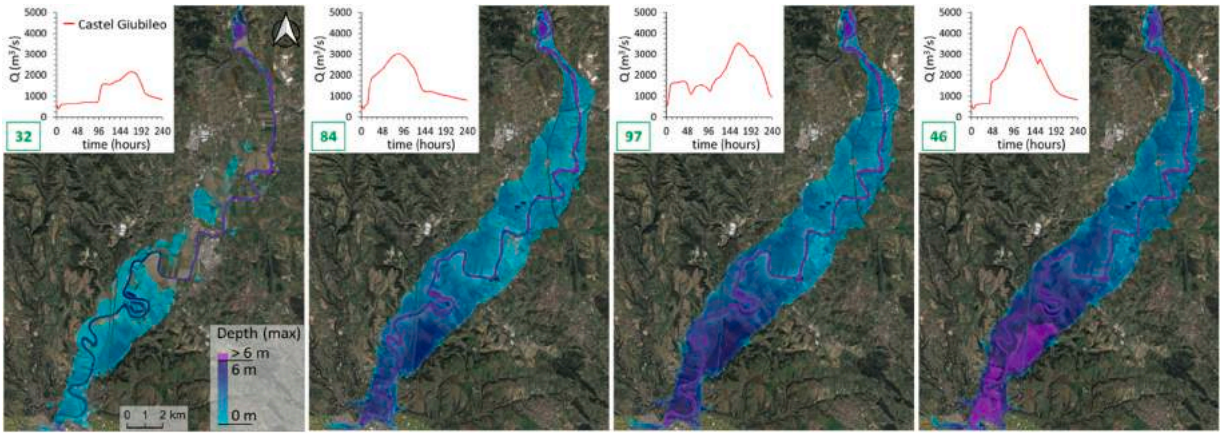

Fig. 7. Results of the 2D model in the MTV for a few noteworthy flooding events: maximum water levels in the Middle Valley for floods N. 32, 84, 97 and 46; the corresponding discharges at Castel Giubileo are depicted in the inserts.

Table 1
Risk distribution in percentage terms the MTV and the city of Rome for the different types of urbanization.

Urbanization type	Annual risk in MTV (%)	Annual risk in Rome (%)
Residential	41	54
Commerce	18	27
Industry	41	6
Office	-	12

periods larger than approximately 40 and 175 years, respectively. An upper limit of $T_r = 500$ years is fixed; since floods with $T_r > 500$ years determine the collapse of the defense structures between Castel Giubileo and the historical town of Rome, with water dynamics that cannot be predicted by the modeling chain that is employed here. Also, the tail of P_Q, i.e. for high return periods, is itself highly uncertainty, characterized by a small number of events.

In the following section we present results for the application of the risk analysis to both the MTV and the city of Rome.

3. Results

3.1. Flood risk in the Middle Tiber Valley (MTV)

Fig. 6 displays the main results of the risk analysis for the MTV, employing the hydrological-hydraulic simulations described in Section 2. In particular, the three panels depict: the cdf P_Q of the peak discharge at the reference section of Castel Giubileo (panel a), the relationship between peak discharge at the reference section and overall damage in the MTV, where a few significant flood events out of the 100 employed are marked in green, with their progressive reference number (panel b), the derived probability distribution of damage in the MTV (panel c). Note that the number of events - out of the 100 floods that inundate the MTV up to $T_r = 500$ years – that are subsequently used for risk computation is 65. The area in blue color in Fig. 6c is equal to the risk R_{MTV}; the aforementioned upper bound for T_r is represented by a dashed line.

The discharge-damage relationship in the MTV (Figure 6~~5~~b) is almost linear, with a slight decrease in slope associated to flow rates around 3500 m^3/s. The damage curve depends on the extension of the flooded areas as represented in the following. Starting from floods with a return period of about forty years (flood n.32 of Fig. 7, that is the 13th out of 100 in terms of increasing peak value), the valley is progressively flooded as T_r increases, involving an increasing number of buildings affected by the flood (flood n. 84, Fig. 7), up to floods with a return time close to five hundred years, when the entire valley is flooded (flood n.97, Fig. 7). Floods with a larger T_r (flood n.46, Fig. 7~~6~~) do not significantly increase the number of buildings as the valley is completely flooded, but only determine an increase in water levels.

The resulting flood risk for the MTV cumulates a value of approximately 5.3 million euro; the distribution of risk for the individual types of urbanization is reported in percentage terms in Table 1. Note that the large part of the urbanization involved by flooding is equally distributed between residential and industrial types, while offices are almost absent. We remind that, by definition, the risk corresponds to the average annual damage produced by the floods in the area measured by euro per year.

3.2. Flood risk in Rome

Fig. 8 shows the main results of the risk analysis for the city of Rome. Like the previous case, the panels show the probability

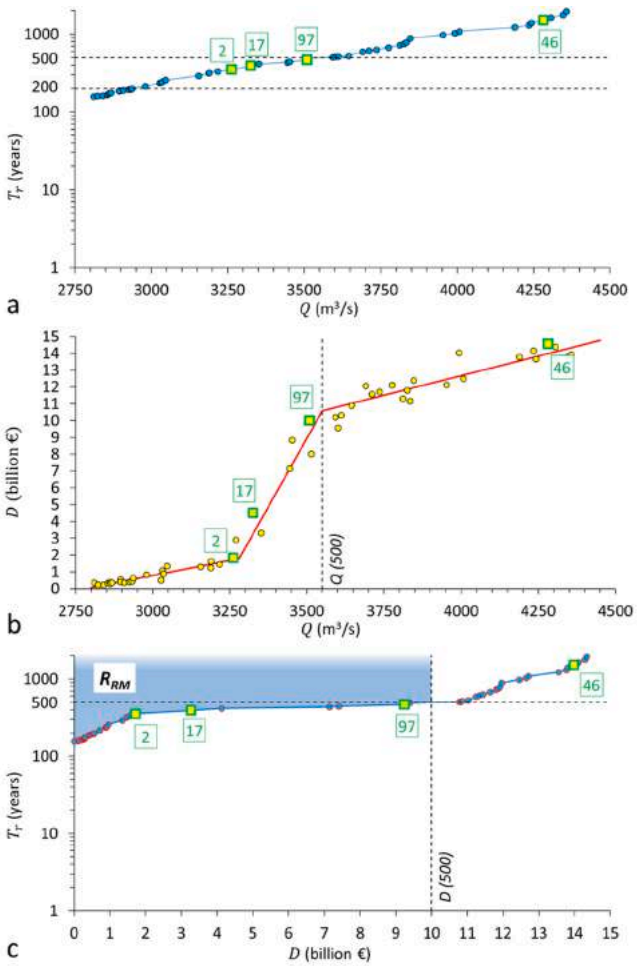

Fig. 8. (a) probability distribution of flood discharge at the Castel Giubileo reference section (equal to Fig. 6a but limited to flood events with return period values exceeding 175 years); (b) empirical flow-damage relationship at Rome; (c) probability distribution of damage at Rome, where the colored area represents the flood risk (i.e. the expected annual damage). Only the events flooding the city of Rome are reported in the figure. A few significant flood events out of the 100 employed are marked in green in all the panels; note also that in panels b and c the vertical dashed line identifies the discharge and damage value corresponding to the maximum return period value considered in the analysis, $T_r = 500$ years.

distribution of the peak discharge at the reference section of Castel Giubileo (panel a, identical to Fig. 6a), the relationship between discharge at the reference section and damage in Rome, where a few significant flood events out of the 100 employed are marked in green, with their progressive reference number (panel b), the derived probability distribution of damage in Rome (panel c). The area in blue color in Fig. 8c is equal to the risk R_{RM}. For consistency with the MVT analysis, the same upper limit $T_r = 500$ years is considered for the risk calculation. We emphasize that, because of the extensive system of levees, damage occurs for flood events with return period larger than around 175 years, i.e. a much larger value of return period than in the MVT. The number of events out of the 100 floods that inundate the city up to $T_r = 500$ years is 31.

Unlike the MVT, the damage-discharge relation in Rome (Fig. 8b) displays three distinct patterns of slope changes: (i) the initial, mild slope results from the (minor) events that do not flood the historic city, mostly because of two major topographical thresholds (near Piazza del Popolo and Piazza Maresciallo Giardino; see flood n. 2 of Fig. 9); (ii) the second segment, with a larger slope, is determined by the events that are able to flood the historic city and, at later stages, the whole city, up to the southern areas named EUR and Via Magliana (flood n. 97, Fig. 9); (iii) the third segment, with a slope similar to the first, can be explained with the same reasons set out in the case of the MVT, i.e. when the town if fully flooded the larger floods lead to increase of water levels only (flood n. 46 of Fig. 9).

The flood risk in Rome (R_{RM}) amounts to approximately 24.3 million euro per year, about four and a half times the flood risk in the MVT. It is worth noting that floods with a return period ranging from approximately 300 to 500 years determine a 5-times increased damage (from 2 to 10 billion euro) which is caused by the progressive flooding of the city (Fig. 8). We remark, once again, that, because of the limited categories of damage considered in this study, the risk R_{RM} provides a lower bound of the flood risk that is expected in Rome. As for the distribution of annual risk by the different urbanization types considered here, it is relevant to stress that half is due to

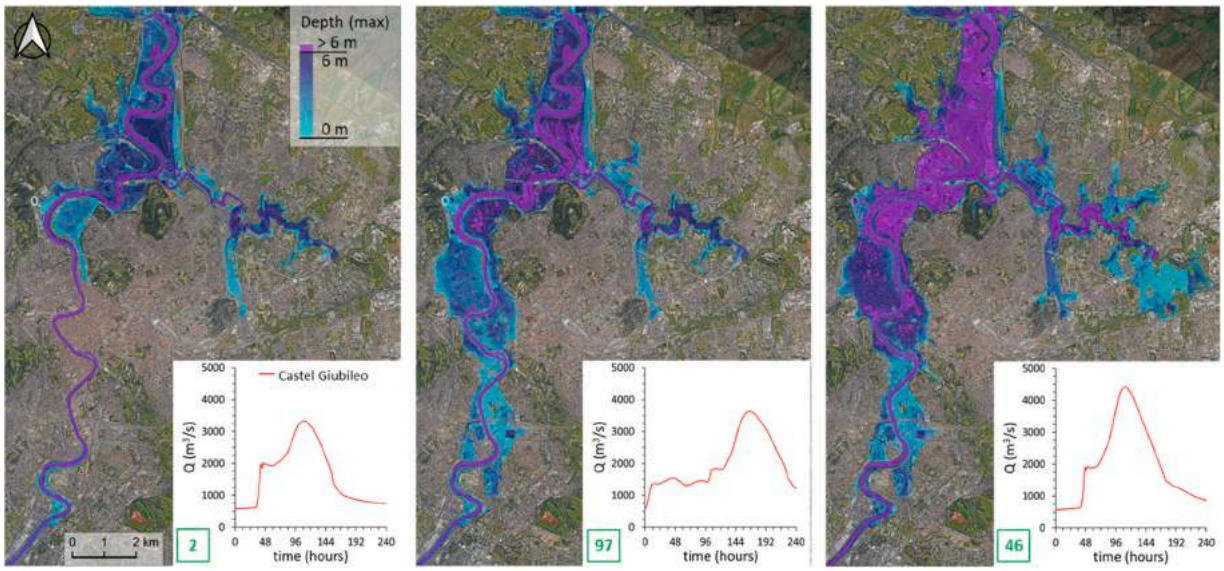

Fig. 9. Results of the 2D model in the town of Rome for a few noteworthy flooding events: maximum water levels for floods N. 2, 97 e 46, approximately characterized by 300, 500 and 1000 years of return period, respectively; the corresponding discharges at Castel Giubileo are depicted in the inserts.

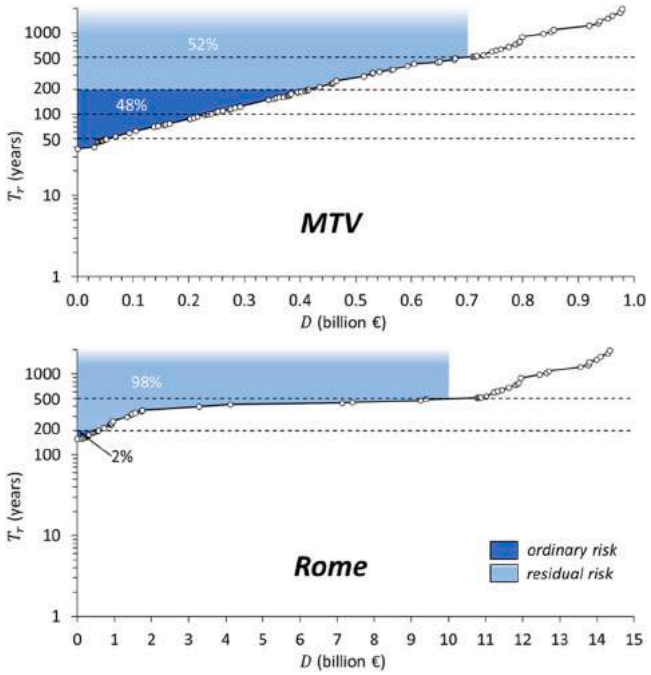

Fig. 10. Ordinary and residual flood risk in the MTV and the city of Rome.

residential urbanization while risk pertaining to commerce, office, and industry is 27%, 12%, and 6%, respectively (Table 1).

4. Discussion

The return period for the design and planning of flood protections measures (e.g. levees) is typical set in Italy as $T_r = 200$ years. The damage associated to floods characterized by $T_r < 200$ years (hereinafter denoted as *ordinary risk*) is considered as "unacceptable", while the management of *residual* risk (i.e. produced by floods with a return period ranging from 200 to 500 years) is deferred to emergency plans, e.g. by civil protection or emergency management agencies. The ordinary risk is nothing else than the *benefit*, or *risk*

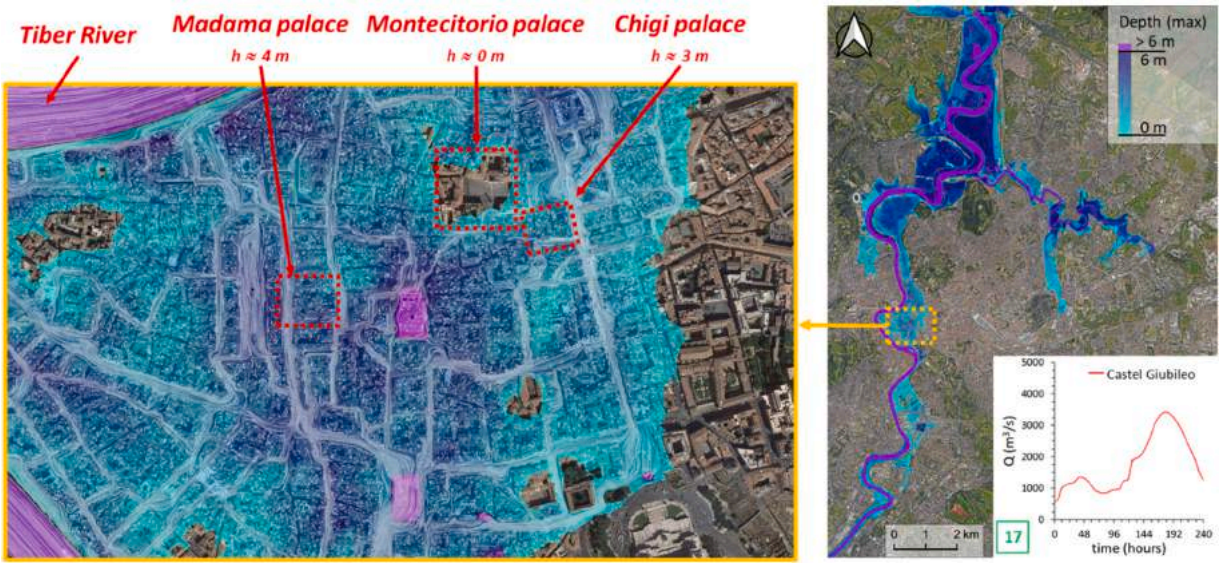

Fig. 11. Modeled maximum water levels in historical Rome for flood n.17, with about T_r= *350 y*; the relative hydrograph, at Castel Giubileo, is depicted in the insert.

reduction, gained by the realization of flood protection works. In the case of levees, the ordinary risk might be straightforwardly represented by the blue shaded area depicted in Fig. 10 (a or b), because the levee construction theoretically tends to fulfill flood protection up to $T_r = 200$ years, when overtopping should start occurring. The corresponding residual risk is represented by the light blue area; this is true if we neglect the effect of levee failure due to other failure mechanisms with respect to overtopping (e.g. piping) increasing the residual risk (the latter could be easily included in the modelling framework considered here, as done by D'Angelo et al., 2020).

Note that in general the shaded areas depict different and variable shapes, depending on the defense measure and on the specific case under analysis. Let's consider, e.g., the effect of a flood detention basin; even if designed with respect to the target flood event with $T_r = 200$ years, the storage usually allows for a suboptimal, partial flood attenuation in a range of T_r values around $T_r = 200$ years (see, e.g., Cipollini et al., 2021). Notwithstanding this, the general definition of ordinary and residual risks remain valid.

More recent Italian legislation, together with the recent "Guidelines for the planning and design of interventions to mitigate hydrogeological risk" (Menduni et al., 2017), highlights that residual risk should be somewhat taken into consideration for the design of effective flood protection measures. Adopting a return period of 200 years in the design may be economically convenient when the ordinary flood risk (i.e. the benefit obtained by the realization of flood protection structures sized for a $T_r = 200$ years return period design event) is far larger than the residual risk, while the cost of the flood protection structures for facing the residual risk would be unbearable. This principle does not apply in the case of the city of Rome, as shown in the following.

Fig. 10 represents the cumulative density function of damage, expressed in terms of return period at the Castel Giubileo section, for both the MTV (Fig. 10a) and Rome (Fig. 10b). As previously stated, the figure displays the ordinary risk, or benefit, ($T_r < 200$ y) and residual risk ($T_r > 200$ y). It is seen that in the MTV the residual risk is about 52% of the ordinary flood risk R_{MTV}; instead, in the city of Rome the residual risk is many times larger than the ordinary risk. Thus, the ordinary risk, that is considered as "unacceptable", is a small fraction of the residual risk, that is supposed to be managed by emergency planning. The situation is even more confusing if we consider that the ordinary risk in Rome would be less than flood risk in the MTV. We remark that floods with a return period exceeding 350 years, that typically have sufficient water volumes to flood the historic center, not only cause significant physical and economical damage but also involve the main Italian government offices (Chamber of Deputies, Senate of the Republic and Presidency of the Council of Ministers), causing governance, public service and business interruptions for several days (an example is given in Fig. 11, that depicts the water levels in central Rome for the flood n.17, with about T_r=*350 y*), not to mention the damage to the cultural and archeological heritage (also not considered in the risk procedure).

In summary, much care should be taken when choosing the reference return period for the flood defense of Rome. The results presented here show that risk-based approach can be very helpful in analyzing the flood protection of sensible areas and the selection of the suitable return period for the design of suitable flood protection measures.

The proposed flood risk-based approach is particularly effective when comparing risk in different areas or in the selection of different flood protection measures. While the assessment of risk is prone to uncertainty, mainly because of the relatively large uncertainties associated with the damage-depth curves and the limitation to direct and tangible damage, useful comparative analyses can be done through the risk ratio between different regions or flood protection scenarios/alternatives. We posit that such risk ratio may provide a more effective quantification of risk than risk itself. For instance, with the rough assumption that risk is underestimated by a certain factor, the latter cancels out when two risk assessments (e.g. for different scenarios) are divided. Thus, the comparison among

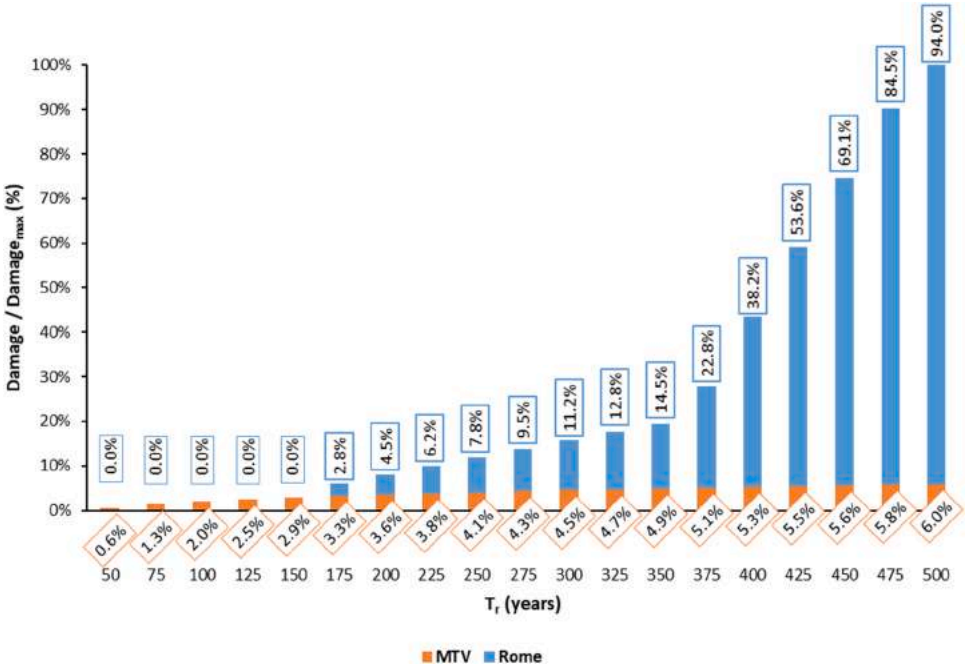

Fig. 12. Normalized damage in the MTV and Rome, $R_{MTV}/(R_{MTV}+R_{RM})$ and $R_{RM}/(R_{MTV}+R_{RM})$, respectively.

regional areas or scenarios helps removing homogeneous biases, yet it might not prevent from scale factors that could impact on the overall risk quantification. As an example, considering the number of people affected, or other peculiar elements that characterize the area (as mentioned in Section 2.4) could exacerbate or attenuate the risk ratio.

A first example is given in Fig. 12 that shows both D_{MTV} and D_{RM}, each normalized with the overall damage $D_{MTV}+D_{RM}$ corresponding to $T_r = 500$ years (denoted as $D_{\max}$), as a function of the return period. The figure shows that the damage in the MTV displays a rather linear slope, from the most frequent floods causing damage (around $T_r = 50$ y), reaching a total of 6% of $D_{\max}$. In Rome, on the other hand, the damage starts at $T_r = 175$ years and grows with a linear slope up to a return period of 350 years; subsequently, the damage in Rome always grows linearly, but with a much larger slope, to reach the 94% of $D_{\max}$. The figure also shows that already for $T_r = 200$ years the damage in Rome exceeds in percentage D_{MTV}. Such type of analysis provides an easy and clear comparison of flood risk among different regions.

Another example deals with the analysis of flood protection scenario, that can be effectively managed by the risk-based procedure. We consider for instance the works that are currently under realization for the protection of the industrial area of the city of Monterotondo (see Fig. 13) from the Tiber River floods. A series of levees around the industrial area of Monterotondo shall protect a total area of 4 km^2 with a design return period of 200 years. Monterotondo is located in the MVT, 15 km from Rome, and the designed levees have likely an influence on the flood frequency of the Tiber River in Rome.

The hydraulic simulations show that, because of the relatively small area defended by the levees, the corresponding increase of water levels in Rome, for a given T_r, will be not significant. Nonetheless, while such increase of water level might be relatively small in absolute terms, it may lead to a significant increase of R_{RM} because of the peculiar shape of the damage-discharge curve (Fig. 8b). In quantitative terms, this planned levee system will lead to a 13.3% increase of R_{RM}, which is rather significant; this result further emphasizes the importance of the MTV in reducing the flood risk in Rome. In turn, the flood risk in the MTV decreases (24.6%) because the complete protection of the Monterotondo area and its assets, up to $T_r = 200$ y. However, such decrease does not compensate the increased R_{RM}, such that the overall risk $R_{MTV}+R_{RM}$ increases of 6.5% after the levee construction. Thus, it is demonstrated that the presented risk analysis is particularly effective in the design and comparative assessment of flood protection measures and their related impact across hydrologic frequency and spatial scales. For this specific case, a flood detention basin is proposed as alternative designed flood mitigation measure, upstream of Monterotondo, to balance the potentially lost flood storage capacity linked to levees, and avoid an increased flood risk for the downstream Rome city center.

5. Conclusions

This work illustrates a flood risk analysis of the city of Rome and the upstream Middle Tiber Valley (MTV). The presented methodological approach moves beyond the standard concept of design flood, demonstrating the performances and benefits of adopting a continuous hydrologic and hydraulic simulation approach (e.g. Grimaldi et al., 2013, 2021). The proposed methodology allows to perform quantitative distributed assessment of inundation impacts associated to a broad spectrum of flood hydrographs generating from varying distributed parametrization of hydrologic forcing conditions for the Tiber River basin, e.g. in terms of flow

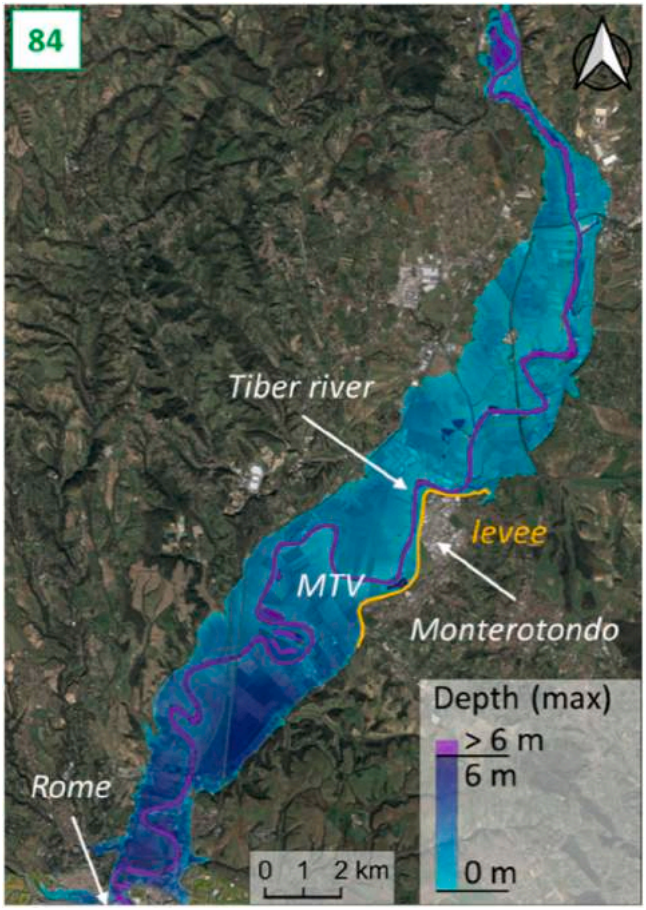

Fig. 13. The industrial area of the city of Monterotondo, where a series of levees protects a total area of 4 km^2 with a design return period of 200 years; Monterotondo is located in the MVT, 15 km from Rome.

peak, flood volume and duration, shape of the hydrograph. The simulations are performed by a hydrological-hydraulic model simulating a long series of annual peak floods, which is the basis for the development of the flood frequency analysis and the derived damage frequency. Flood risk is evaluated through the procedure proposed by Huizinga et al. (2017), where only direct and tangible damages are considered. Therefore, the derived risk represents an underestimation of the total risk, that typically includes other sources of damage (i.e. direct and intangible, and indirect). To our knowledge this is the first time that a quantification - albeit simplified - of the flood risk of Rome and the upstream Tiber valley is carried out, as well as the first study to adopt continuous-simulation methodology in the same area for flood-damage analyses.

Results show how the damage in the MTV starts for floods with a return period of about 40 years, then growing linearly up to floods of about 500 years return period, for which a damage of several hundred million euro is attained. In the city of Rome damage begins with floods with $T_r = 175$ years, which generate damage of hundreds of million euro, and grow linearly up to floods with a return period of around 350 years, for which the majority of the historical town is flooded; then it keeps growing with a greater slope to reach a damage of about ten billion euros for $T_r = 500$ years flood events.

As expected, the flood risk of Rome is much larger than the flood risk in the MTV for flood events with a return period larger than 200 years. At the same time, the flood dynamics in the MTV are crucial for the mitigation of flood in Rome, such that any change of land use in the valley must be studies to verify the downstream effects. To this matter, the risk-based approach (although approximated and affected by uncertainties) proves to be particularly effective in the design and evaluation of flood protection measures and their impact across scales. In particular, it was shown how risk analyses provide useful comparisons of flood conditions and scenarios by taking the ratio of the respective flood risks. We advocate that such “comparative” use of flood risk is rather effective, somewhat mitigating the high level of uncertainty always present in the risk calculation.

Finally, the presented flood risk assessments highlight how quantitative residual risk metrics in Rome are fundamental for a correct definition of the design return period for any suitable flood protection measure, in both the city of Rome and the upstream MTV.

We conclude by emphasizing the uncertainties associated to the flood risk calculation; they derive from all the components of the modeling chain, starting from the hydrological analysis to arrive at the definition of damage, which is probably the most difficult and error prone component of the methodology. Hence, we believe that the current analyses of flood risk may at best provide an order of

magnitude of risk, and more research is needed in order to refine the existing methods and make them more generalizable, including other important sources of damage (e.g. indirect costs). Nevertheless, we surmise that the flood risk analysis may be quite effective when comparing different situations, or technical solutions, and help in the design of flood protection infrastructures and the management of the territory.

CRediT authorship contribution statement

A.Fiori: Conceptualization, Methodology, Writing – Original Draft. **C.P. Mancini**: Conceptualization, Methodology, Data curation, Software, Visualization, Supervision. **A. Annis**: Methodology, Software, Investigation, Visualization, Data Curation. **S. Lollai**: Software, Investigation, Visualization, Data Curation. **E.Volpi**: Conceptualization, Methodology, Formal Analysis, Writing - Review & Editing, Software. **F.Nardi:** Conceptualization, Methodology, Writing- Reviewing and Editing. **S.Grimaldi:** Conceptualization, Methodology, Writing- Reviewing and Editing.

Declaration of Competing Interest

The authors declare the following financial interests/personal relationships which may be considered as potential competing interests: All authors reports financial support was provided by Prologis.

Data Availability

The data that has been used is confidential.

Acknowledgements

The financial contribution of PROLOGIS applied research project (Grant agreement no. 7209) to Roma Tre University, University for Foreigners of Perugia and University of Tuscia is gratefully acknowledged in support of this publication. The Authors sincerely thanks the Associate Editors and four anonymous Reviewers for the faithful comments that helped improved the quality of our work.

References

ABDAC, 2003. Assetto Idraulico della Media valle del Tevere tra l'invaso di Corbara e la traversa di Castel Giubileo e indirizzi operativi per l'intero bacino, Roma.
Annis, A., Nardi, F., Volpi, E., Fiori, A., 2020. Quantifying the relative impact of hydrological and hydraulic modelling parameterizations on uncertainty of inundation maps. Hydrol. Sci. J. 65 (4), 507–523.
Annis, A., Nardi, F., Castelli, F., 2022. Simultaneous assimilation of water levels from river gauges and satellite flood maps for near-real-time flood mapping. Hydrol. Earth Syst. Sci. 26 (4), 1019–1041.
Arrighi, C., Brugioni, M., Castelli, F., Franceschini, S., Mazzanti, B., 2013. Urban micro-scale flood risk estimation with parsimonious hydraulic modelling and census data. Nat. Hazards earth Syst. Sci. 13 (5), 1375–1391.
Bates, P.D., 2022. Flood inundation prediction. Annu. Rev. Fluid Mech. 54, 287–315.
Bell, H., Tobin, M., 2007. Efficient and effective? The 100-year flood in the communication and perception of flood risk. Environ. Hazards 7, 302–311.
Beneyto, C., Aranda, J.Á., Benito, G., Francés, F., 2020. New approach to estimate extreme flooding using continuous synthetic simulation supported by regional precipitation and non-systematic flood data. Water 12 (11), 3174.
Boughton, W., Droop, O., 2003. Continuous simulation for design flood estimation—a review. Environ. Model. Softw. 18 (4), 309–318.
Brunner, G.W., 2016. HEC-RAS river analysis system, 2D modeling user's manual. Version 5.0. In Davis: US Army Corps of Engineers; Hydrologic Engineering Center, Davis, CA, USA.
Calenda, G., Mancini, C.P., Volpi, E., 2009. Selection of the probabilistic model of extreme floods: the case of the River Tiber in Rome. J. Hydrol. 371, 1–11, 10.1016.
Cipollini, S., Fiori, A., Volpi, A., E., 2021. Structure-based framework for the design and risk assessment of hydraulic structures, with application to offline flood detention basins. J. Hydrol. 600, 126527.
D'Angelo, C., Fiori, A., Volpi, E., 2020. Structural, dynamic and anthropic conditions that trigger the emergence of the levee effect: insight from a simplified risk-based framework. Hydrol. Sci. J. 65 (6), 914–927.
European Parliament and of the Council of 23 October 2007. Directive 2007/60/EC on the assessment and management of flood risks.
Falter, D., Schröter, K., Dung, N.V., Vorogushyn, S., Kreibich, H., Hundecha, Y., Merz, B., 2015. Spatially coherent flood risk assessment based on long-term continuous simulation with a coupled model chain. J. Hydrol. 524, 182–193.
Fleischmann, A.S., Collischonn, W., Paiva, R.C.D.D., 2019. Estimating design hydrographs at the basin scale: from event-based to continuous hydrological simulation. RBRH 24.
Galloway, G., cited in Armah, J., H. Ayan, C., Bernard, A., Blumenhal, L., Fortmann, L.R., Garretson, C., Goodwin, W.D., Runolfson, T.B., Davis, J. Vano, and R.O. Zerbe Jr, 2005 2009. Principles and guidelines for evaluating federal water projects: U.S. Army Corps of Engineers planning and the use of benefit cost analysis: A report for the Congressional Research Service. Evans School of Public Affairs, University of Washington, (Accessed 31 October 2014) at http://fas.org/irp/agency/dhs/fema/evans.pdf.
Galloway, G.E., Seminara, G., Blöschl, G., García, M.H., Montanari, A., Solari, L., 2020. Reducing the flood risk of art cities: the case of Florence. J. Hydraul. Eng. 146 (5), 02520001.
Grimaldi, S., Petroselli, A., Serinaldi, F., 2012. Design hydrograph estimation in small and ungauged watersheds: Continuous simulation method versus event-based approach. Hydrol. Process. 26 (20), 3124–3134.
Grimaldi, S., Petroselli, A., Arcangeletti, E., Nardi, F., 2013. Flood mapping in ungauged basins using fully continuous hydrologic–hydraulic modeling. J. Hydrol. 487, 39–47.
Grimaldi, S., Nardi, F., Piscopia, R., Petroselli, A., Apollonio, C., 2021. Continuous hydrologic modelling for design simulation in small and ungauged basins: a step forward and some tests for its practical use. J. Hydrol. 595, 125664 (art. No).
Grimaldi, S., Volpi, E., Langousis, A., Papalexiou, S., De Luca, D., Piscopia, R., Nerantzaki, S.D., Papacharalampous, G., Petroselli, A., 2022. Continuous hydrologic modelling for small and ungauged basins: a comparison of eight rainfall models for sub-daily runoff simulations. J. Hydrol. 610, 127866 (art. no).
Hoes, O., Nelen, F., 2005. Continuous simulation or event-based modelling to estimate flood probabilities? WIT Trans. Ecol. Environ. 80.

Huizinga, J., de Moel Hans, H., Szewczyk, W., 2017. Joint research centre, technical reports, European Commission. Glob. flood depth - Damage Funct., Methodol. Database Guidel.
Ludy, J., Kondolf, G.M., 2012. Flood risk perception in lands "protected" by 100-year levees. Nat. Hazards 61, 829–842.
Mancini, C.P., Lollai, S., Calenda, G., Volpi, E., Fiori, A., 2022. Guidance in the calibration of two-dimensional models of historical floods in urban areas: a case study. Hydrol. Sci. J. 67 (3), 358–368.
Menduni, G., Brath, A., Iannelli, E., Zarra, C., 2017. Linee guida per le attività di programmazione e Progettazione degli interventi per il contrasto del rischio idrogeologico. #Italia Sicura, Presidenza del Consiglio dei Ministri. Associazione Idrotecnica Italiana, ISBN, 9788894874006.
Merz, B., Blöschl, G., Vorogushyn, S., Dottori, F., Aerts, J.C., Bates, P., Macdonald, E., 2021. Causes, impacts and patterns of disastrous river floods. Nat. Rev. Earth Environ. 2 (9), 592–609.
Metin, A.D., Dung, N.V., Schröter, K., Vorogushyn, S., Guse, B., Kreibich, H., Merz, B., 2020. The role of spatial dependence for large-scale flood risk estimation. Nat. Hazards Earth Syst. Sci. 20 (4), 967–979.
Molinari, D., Scorzini, A.R., Arrighi, C., Carisi, F., Castelli, F., Domeneghetti, A., Ballio, F., 2020. Are flood damage models converging to "reality"? Lessons learnt from a blind test. Nat. Hazards Earth Syst. Sci. 20 (11), 2997–3017.
Paprotny, D., Kreibich, H., Morales-Nápoles, O., Wagenaar, D., Castellarin, A., Carisi, F., Schröter, F., K., 2021. A probabilistic approach to estimating residential losses from different flood types. Nat. Hazards 105, 2569–2601.
Pinter, N., Huthoff, F., Dierauer, J., Remo, J.W., Damptz, A., 2016. Modeling residual flood risk behind levees, Upper Mississippi River. Usa. *Environ. Sci. Policy* 58, 131–140.
SwissRe (2023) last accessed, February 27th, 2023 https://www.swissre.com/dam/jcr:cd31e6de-c068–402e-9767–76d92a1444ef/factsheet_riskycities_rome_web.pdf.
UNISDR (2009) Terminology on disaster risk reduction. Geneva.
Varnes, D.J., 1984. Landslide hazard zonation: A review of principles and practice. IAEG Monograph. UNESCO, p. 59.
Volpi, E., Fiori, A., 2012. Design event selection in bivariate hydrological frequency analysis. Hydrol. Sci. J. 57 (8), 1506–1515.